Polyhedron 228 (2022) 116179

Contents lists available at ScienceDirect

Polyhedron

journal homepage: www.elsevier.com/locate/poly

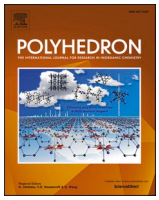

Aryl, bi-functionalised imidazo[4,5-*f*]-1,10-phenanthroline ligands and their luminescent rhenium(I) complexes

R. Owen Bonello [a], Mateusz B. Pitak [b], Graham J. Tizzard [b], Simon J. Coles [b], Ian A. Fallis [a,*], Simon J.A. Pope [a,*]

[a] *School of Chemistry, Main Building, Cardiff University, Museum Avenue, Cardiff CF10 3AT, United Kingdom*
[b] *UK National Crystallographic Service, Chemistry, Faculty of Natural and Environmental Sciences, University of Southampton, Highfield, Southampton, England SO17 1BJ, United Kingdom*

A B S T R A C T

Five new imidazo[4,5-*f*]-1,10-phenanthroline based ligands (**1**–**5**) have been synthesised and characterised. The facile synthesis of **1**–**5** allows two regiochemical points of structural variety allowing highly conjugated and bulky aryl groups of varying functionalities, including azobenzene, trityl and terpyridine constituents, to be attached to the ligand core. **1**–**5** are fluorescent (λ_{em} = 410–415 nm), and react readily with [ReBr(CO)$_5$] in toluene to give neutral coordination complexes of the form *fac*-[ReBr(CO)$_3$(**1**–**5**)]. The series of complexes was characterised using a variety of spectroscopic and analytical techniques. Two examples of this series were characterised in the solid state using single crystal X-ray diffraction which confirmed the octahedral geometry and formulation. Photophysical studies showed that *fac*-[ReBr(CO)$_3$(**1**–**5**)] are phosphorescent in solution under ambient conditions, revealing visible emission (558–585 nm) in aerated solution with corresponding lifetimes in the range 149–267 ns. These attributes are consistent with a triplet metal to ligand charge transfer (^{3}MLCT) emitting state.

1. Introduction

2,4,5-triphenylimidazole [1] (lophine) based chromophores are a very well-known class of molecule [2] which are of interest in several areas of application due to their fluorescence and chemiluminescence properties [3]. Various synthetic approaches have been described [4] and the fluorescent properties of these species can be altered via the addition of different groups to the imidazole core [5]. Because of the convenient syntheses that have been described for such species, it is also possible to deploy these interesting molecular systems in the context of ligands for coordination chemistry. For example, imidazo[4,5-*f*]-1,10-phenanthroline derivatives, where the chelating unit is integrated into the 2,4,5-triarylimidazole core, continue to attract attention as they can be easily adapted for coordination chemistry [6], as well as a variety of other potential applications [7].

Ru(II) complexes incorporating imidazo[4,5-*f*]-1,10-phenanthroline type ligands have been investigated because of interest in their excited state properties [8], light harvesting attributes [9], and biological application [10], including DNA binding [11] and anti-cancer properties [12]. Photodynamic antitumoural activity has also been noted with Ru(II) complexes based on imidazo[4,5-*f*]-1,10-phenanthroline derivatives that integrate an apical hydroxybenzoic acid group [13]. Fluorescence cell imaging studies have shown that similar Ru(II) complexes have mitochondrial targeting behaviour and have thus been postulated as anti-cancer agents [14].

Imidazo[4,5-*f*]-1,10-phenanthroline derived ligands have also been complexed with a range of other metal ions including Ir(III) [15], Pt(II) [16], Cu(I) [17], and Co(II) [18]. The luminescent properties of Ir(III) complexes can be enhanced through the use of these ligands. For example, a coumarin conjugated imidazo[4,5-*f*]-1,10-phenanthroline complex has shown enhanced excited triplet state lifetimes which are advantageous for energy upconversion performance [19]. Related Ir(III) systems have also shown good two-photon excitation properties [20], as well as aggregation-induced phosphorescence [21,22] allowing investigations using bioimaging. With judicious choice of functionality, polydenticity can also be imparted upon these types of ligands allowing applications in coordination polymers with trivalent lanthanides [23] and work towards complexes with interesting magnetic properties [24].

In addition to our own contributions [25], the reports of imidazo[4,5-*f*]-1,10-phenanthroline complexes with Re(I) are far less extensive, but examples have been described [26]. These include recent work on aggregation-induced emission using 2-(2-thienyl)imidazo[4,5-*f*]-1,10-phenanthroline species [27], and complexes for use in colourimetric and fluorimetric based sensors [28]. In this current work we describe the synthesis and investigation of a range of new imidazo[4,5-*f*]-1,10-phenanthroline ligands which incorporate two different R groups (one on

* Corresponding authors.
E-mail addresses: fallis@cardiff.ac.uk (I.A. Fallis), popesj@cardiff.ac.uk (S.J.A. Pope).

https://doi.org/10.1016/j.poly.2022.116179
Received 28 July 2022; Accepted 14 October 2022
Available online 20 October 2022

the apical site and one linked to the nitrogen in the imidazole-like ring) giving multi-functionality. The possibility of introducing bulky aryl groups such as trityl, azodye substitutents and a pendant terpyridine unit into a phosphorescent complex were investigated. These different types of ligand substituent were of interest because of the potential future work that could be envisaged, including highly lipophilic complexes for bioimaging studies, and building blocks for multimetallic photoactive assemblies.

2. Synthesis and characterisation of the ligands

The syntheses of the imidazo[4,5-*f*]-1,10-phenanthroline-based ligands (Scheme 1) was achieved using an adaption of a previously reported methodology [25]. A one-pot synthetic approach in acetic acid, wherein a combination of aryl amines (**S2-NH$_2$**) and aldehydes (**S1-CHO**) reagents were investigated. This approach proved tolerant to a range of highly functionalised and bulky aryl substituents. For example, an anilino azobenzene, the highly lipophilic 4-tritylaniline, and 4-([2,2′:6′,2′′-terpyridin]-4′-yl)aniline were all compatible with this synthetic approach, thus yielding highly functionalised ligands; **5** was isolated from 4-(benzoyloxy)benzaldehyde. In general, the substituted imidazo[4,5-*f*]-1,10-phenanthroline ligands (**1**–**5**) were typically isolated as off-white solids, with the exception of the azobenzene derivatives (**2**, **3**), which were obtained as light orange powders. All species displayed poor solubility in water, but good solubility in a range of common organic solvents.

The characterisation of compounds **1**–**5** was initially investigated using ^{1}H and ^{13}C{^{1}H} NMR spectroscopies. The incorporation of different aromatic substituents and the unsymmetrical nature of **1**–**5** generally led to detailed ^{1}H NMR spectra, particularly in the aromatic region. However, characteristic peaks were often identified allowing confirmation of the proposed structures. For example, the ^{1}H NMR spectrum of **1** displayed a singlet at 1.27 ppm consistent with the butyl moiety, and two furthest downfield doublets (at 9.22 and 9.18 ppm) consistent with the protons at the 2- and 9-positions of the phenanthroline group; this latter pattern was typically observed for **1**–**5**. The ^{1}H NMR spectra of **2** showed two singlets at 3.78 and 3.83 ppm consistent with the inequivalent methoxy groups of the apical substituent. **5** revealed a singlet at 2.43 (6H integral) suggesting free rotation of the ring, while the ^{13}C{^{1}H} NMR spectrum clearly identified the C═O resonance at 164.9 ppm consistent with retention of the ester functionality within the ligand structure (Fig. S1, ESI). **1**–**5** were further characterised using HRMS, IR and UV–vis. absorption spectroscopies (see later discussion). Full characterisation details are presented in the Experimental section.

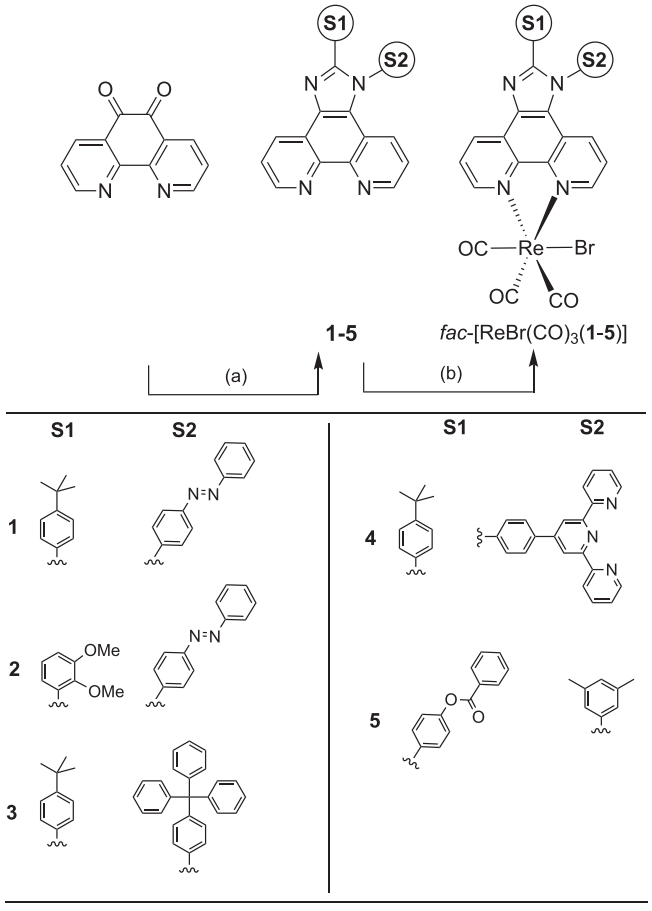

Scheme 1. Route to the new ligands and complexes: (a) S1-CHO, S2-NH$_2$, AcOH, heat; (b) [ReBr(CO)$_5$], toluene, heat.

3. Synthesis and characterisation of the Re(I) complexes

The coordination chemistry of the ligands (**1**–**5**) was investigated by reaction with [ReBr(CO)$_5$] using standard conditions (toluene, heat, 24 hr) to yield the expected complexes, *fac*-[ReBr(CO)$_3$(**1**–**5**)], as air-stable, yellow-orange coloured solids. All isolated compounds (Scheme 2) were initially investigated by ^{1}H and ^{13}C{^{1}H} NMR spectroscopies (where solubility permitted). Across the series, the successful chelation of the ligands was evident by downfield shifts in the unique proton resonances associated with the unsymmetrical phenanthroline chelate.

For example, comparison of the spectra of **5** and *fac*-[ReBr(CO)$_3$(**5**)] showed approximately + 0.2 ppm shifts of the phenanthroline protons (particularly clear for resonances > 9 ppm) together with smaller shifts for the other aromatic protons (see Fig. 1). Interestingly, while the ^{1}H NMR spectrum of ligand **5** revealed equivalent methyl groups (at 2.43 ppm) associated with the dimethylaniline group (implying free rotation of the substituent), the corresponding spectrum for *fac*-[ReBr(CO)$_3$(**5**)] suggested a subtle inequivalence imparted by complexation with Re(I). Two singlets were observed at 2.48 and 2.50 ppm, both of which are slightly downfield from the corresponding resonance in **5** and therefore implies an inhibition of rotation of that substituent once the ligand is coordinated. Characteristic aliphatic resonances were also indicative of the successful formation of *fac*-[ReBr(CO)$_3$(**2**)], where the two methoxy resonances showed a subtle downfield shift from the free ligand to 3.71 and 3.77 ppm. In most cases, and where solubility allowed, ^{13}C{^{1}H} NMR spectra were used to identify three downfield resonances *ca.* 189–197 ppm, which correspond to the coordinated carbonyl ligands. In the case of *fac*-[ReBr(CO)$_3$(**5**)] these downfield resonances were supplemented by the ester carbonyl of the ligand at 164.9 ppm.

The ^{1}H NMR spectrum of the terpyridine adorned *fac*-[ReBr(CO)$_3$(**4**)] could only be acquired in d6-DMSO due to limited solubility in other common NMR solvents. Comparison of the spectrum with that of the free ligand (**4**) showed significant shifts in some of the peaks which indicated coordination of the rhenium centre. Hypothetically, there are two sites of coordination: the 1,10-phenanthroline or the 2,2′:6′,2′′-terpyridine unit (previous studies have shown that under relatively mild conditions 2,2′:6′,2′′-terpyridine species are likely to coordinate to Re(I) in a bidentate fashion) [29]. For *fac*-[ReBr(CO)$_3$(**4**)], the NMR data showed, through comparison with the other complexes, that the furthest downfield shifts were those associated with the 1,10-phenanthroline moiety, and therefore suggestive as the most likely site of complexation (rather than the terpyridine terminus). Finally, the presence of only one signal for the aliphatic *tert*-butyl group was consistent with the formation of a single complex species with one coordination mode.

Solid-state IR spectroscopic studies were also undertaken on the complexes to reveal either two or three ν(C═O) bands between 2050 and 1850 cm^{-1}, the two lower frequency absorptions occasionally overlapping around 1920–1880 cm^{-1} (e.g. Fig. 2). This is consistent

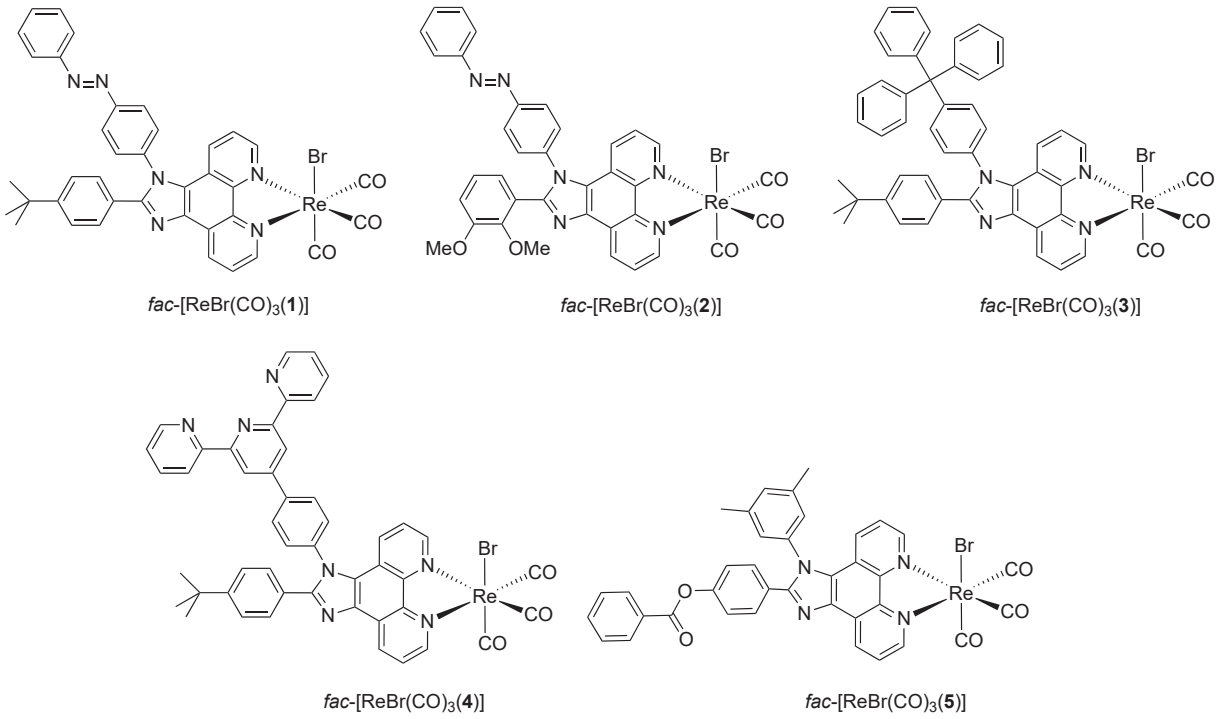

Scheme 2. Structures of the isolated complexes.

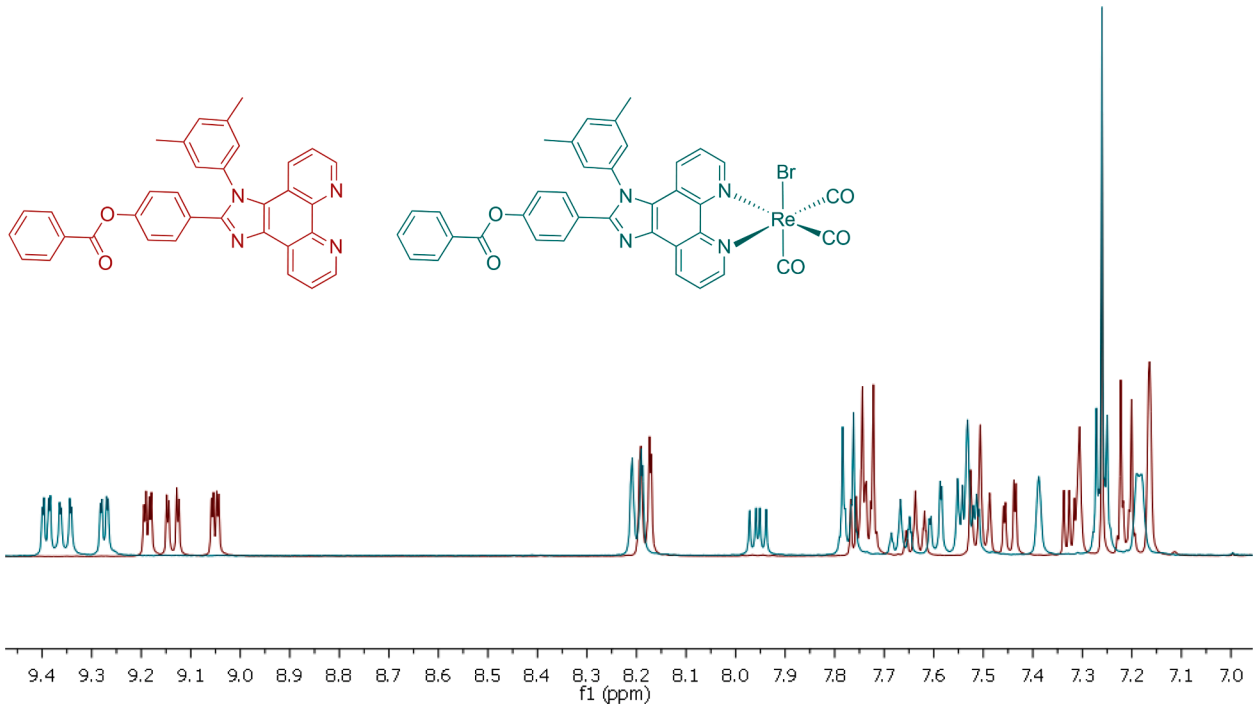

Fig. 1. A comparison of the ^{1}H NMR spectra of the aromatic region of ligand **5** (red) and the corresponding complex *fac*-[ReBr(CO)$_3$(**5**)] (blue) in $CDCl_3$ at 298 K. ((Colour online.))

with a local symmetry (with respect to the coordinated carbonyl ligands) that can be approximated to a C_s point group, as expected [25] for the facially capped coordination geometry at Re(I). *fac*-[ReBr(CO)$_3$(**5**)], which contains the benzoate group also displayed the characteristic peaks that were observed in the free ligand, with the C═O ester group visible at around 1700 cm^{-1} (Fig. 2). High resolution mass spectrometry data was obtained for all complexes revealing the protonated parent ion (e.g. Fig. 3) or cationic sodium adduct in each case.

4. X-ray crystal structures of the complexes

Suitable crystals of two complexes, *fac*-[ReBr(CO)$_3$(**1**)] and *fac*-[ReBr(CO)$_3$(**5**)], were obtained by the slow diffusion of hexane into a toluene solution of the complex, allowing single crystal X-ray diffraction studies to be undertaken. The parameters associated with the data collection for both complexes are shown in Table S1, with selected bond length and angle data in the corresponding figure captions. *fac*-[ReBr(CO)$_3$(**5**)]

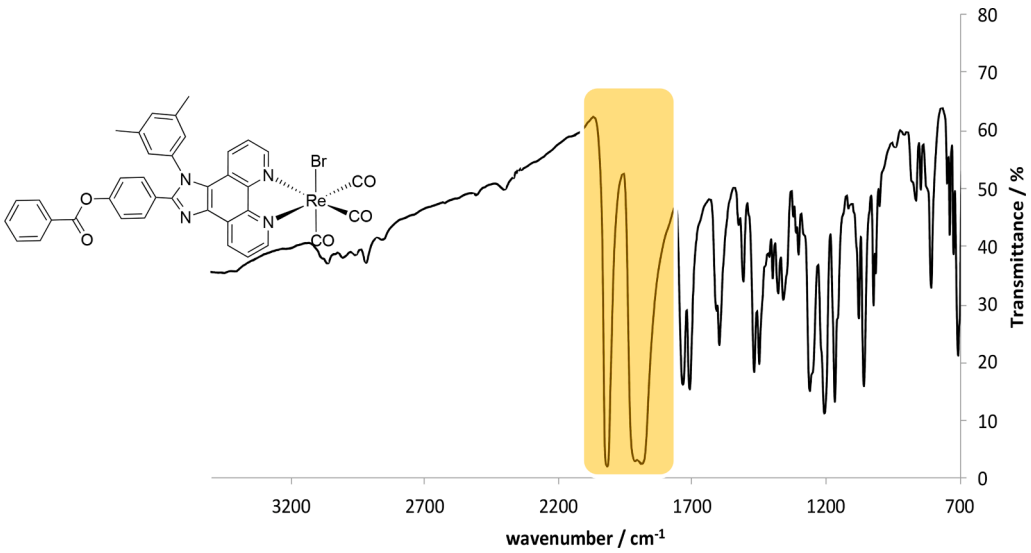

Fig. 2. IR spectrum (KBr disc) of complex *fac*-[ReBr(CO)$_3$(**5**)], with ν(C$\equiv$O) highlighted.

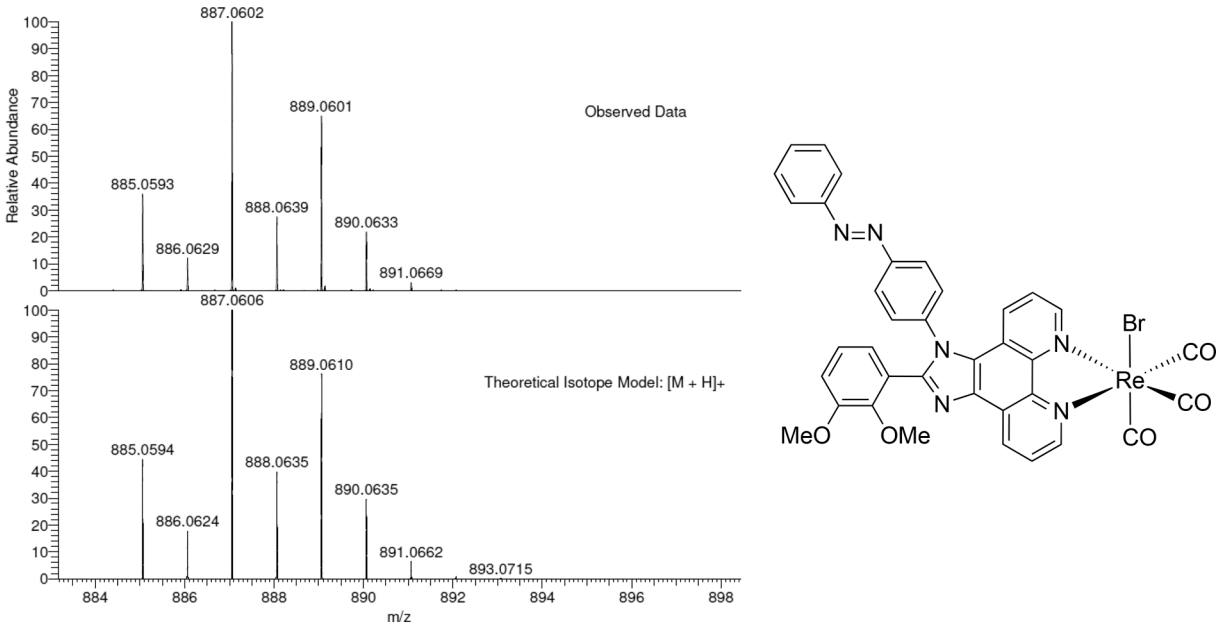

Fig. 3. HR MS data for complex *fac*-[ReBr(CO)$_3$(**2**)] showing a comparison between experimental and theoretical isotopic distributions consistent with *m/z* for [M + H]$^+$.

crystallised as the toluene solvate.

Both X-ray structures (Figs. 4 and 5) show the anticipated mode of coordination for the ligands, chelating *trans* to the two carbonyl ligands, with the third CO ligand and bromide donors occupying the axial positions at the Re atoms. All bond lengths and angles associated with the coordination sphere are typical for a [ReBr(CO)$_3$(N^N)] type complex with a chelating diimine [25,30]. For both structures, the steric congestion arising from the 1,2-diaryl substituted imidazole groups results in these groups mutually rotating away from planarity to the ligand core. The apical *p*^{t}butylphenyl substituent of *fac*-[ReBr(CO)$_3$(**1**)] deviates from planarity by a torsion angle of 35.3(2)°, whilst the proximal 4-substituted aryl group of the azobenzene sidearm has a torsion angle of 77.4(2)° and is observed in its lower energy *E*-configuration. Interestingly, the distal phenyl group of the azobenzene moiety is approximately co-planar with the ligand core. The structure of *fac*-[ReBr(CO)$_3$(**5**)] is observed with the 4-benzoyloxyphenyl group displaying a torsion angle of 41.86(12)° relative to the ligand core and the distal phenyl ring of the benzolyloxy moiety being approximately co-planar to the imidazo[4,5-*f*]-1,10-phenanthroline core. The R′ group, 3,5-dimethylphenyl, displays a torsion angle of 71.69(12)°. In the case of *fac*-[ReBr(CO)$_3$(**1**)] no significant contacts were observed in the packing diagram whilst with *fac*-[ReBr(CO)$_3$(**5**)] an approximately graphitic slipped π-stacking interaction (3.558(10) Å) was observed between adjacent 4-substituted aryl groups of the 4-benzoyloxyphenyl moieties.

5. UV–vis Absorption and luminescence spectroscopy

Firstly, chloroform solutions of the free ligand **1**–**5** were investigated using UV–vis. absorption spectroscopy. Generally, the electronic spectra of **1**–**5** showed a composite of bands in the UV region with large molar absorption coefficients ($\varepsilon > 3 \times 10^4$ M^{-1} cm^{-1}). These various bands are therefore likely to be associated with different allowed $\pi \rightarrow \pi^*$ transitions within the aromatic components of the ligands. The spectra for the azo derivatives **1** and **2** show stronger absorption between 350 and 400

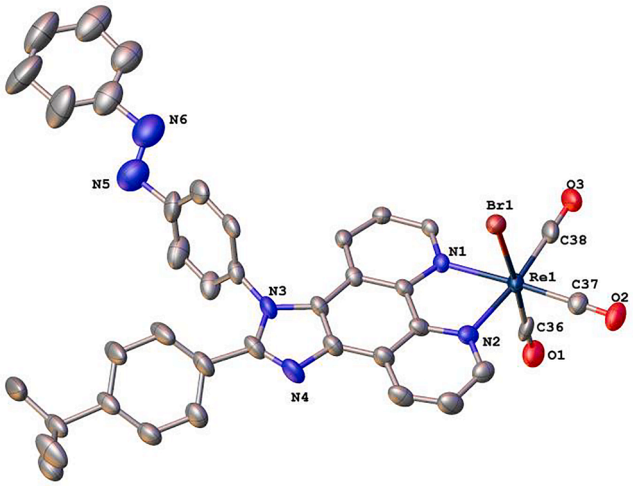

Fig. 4. X-ray structure of complex *fac*-[ReBr(CO)$_3$(**1**)] with hydrogen atoms and toluene solvate solvent molecules (toluene) omitted for clarity. Selected data - bond lengths (Å): C36–Re1, 1.964(8); C37–Re1, 1.920(7); C38–Re1, 1.908(7); N1–Re1, 2.184(5); N2–Re1, 2.177(5); Br1–Re1, 2.6119(7). Bond angles (°): O2–C37–Re1, 178.5(6); O3–C38–Re1, 179.0(7); C1–N1–Re1, 125.6(4); C5–N1–Re1, 115.2(4); C12–N2–Re1, 125.6(4); C9–N2–Re1, 114.9(4); C37–Re1–C38, 87.4(3); C37–Re1–C36, 88.7(3); C38–Re1–C36, 91.9(3); C37–Re1–N2, 98.8(2); C38–Re1–N2, 172.6(2); C36–Re1–N2, 92.2(2); C37–Re1–N1, 173.6(2); C38–Re1–N1, 98.1(2); C36–Re1–N1, 94.3(2); N2–Re1–N1, 75.44(18); C37–Re1–Br1, 93.9(2); C38–Re1–Br1, 91.0(2); C36–Re1–Br1, 176.18(19); N2–Re1–Br1, 84.67(13); N1–Re1–Br1, 82.85(12). ADP ellipsoids are displayed at 50 % probability.

nm and a weaker shoulder at 400–450 nm may be attributed to the presence of a formally $n \rightarrow \pi^*$ transition localised within the azobenzene moiety of these species (Fig. 6).

Ligands **1**–**5** were then investigated using steady state and time-resolved luminescence spectrocopy. Following excitation in the UV region, each of the ligands demonstrated emission in the blue part of the visible region at 415 (for ligand **1**), 414 (**2**), 414 (**3**), 415 (**4**) and 403 nm (**5**). The spectral appearance of the emission bands often revealed a hint of vibronic coupling (e.g. Fig. 6) typical of a $^1(\pi\text{-}\pi^*)$ excited state in a rigid chromophore. The invariance of the emission maxima suggests that the imidazo[4,5-*f*]-1,10-phenanthroline core is primarily responsible for the emission properties, which is consistent with a lack of extended conjugation arising from the differing substituents. With associated emission lifetimes (λ_{ex} = 295 nm) of 3.7, 3.6, 3.7, 3.6, and 2.6 ns, for **1**–**5** respectively, these results also indicate emission from a spin-allowed relaxation process (i.e. fluorescence) in each case which probably originates from a $^1(\pi\text{-}\pi^*)$ excited state.

The UV–vis. absorption properties of the Re(I) complexes showed a range of bands in the UV and visible regions. Typically, the shorter wavelength features were associated with the expected intraligand transitions (mainly originating from $\pi \rightarrow \pi^*$ transitions discussed earlier) that are affiliated with the different aromatic constituents within the ligand framework. For example, *fac*-[ReBr(CO)$_3$(**3**)] has a relatively intense feature at 274 nm which can be attributed to the summative absorption of the trityl unit with the core of the ligand (Fig. 7). In the visible region a new, characteristically broad peak at 400–500 nm is apparent for the complexes (e.g. Figs. 7 and 8) and is consistent with a metal-to-ligand charge transfer ($M_{Re}LCT$) transition, in accordance with numerous previous studies on diimine complexes of Re(I) [31]. The magnitude of the molar absorption coefficients (typically ~ 7000 M^{-1} cm^{-1}) suggests a spin-allowed process (i.e. $S_0 \rightarrow S_1$) associated with this $M_{Re}LCT$ transition. It is also possible that a spin forbidden transition (^{3}MLCT; $S_0 \rightarrow T_1$) may contribute to the weaker, lower energy shoulder of this absorption band, as has been noted in other heavy metal complexes (for example, those based upon iridium) that possess significant spin orbit coupling [32]. In two cases, *fac*-[ReBr(CO)$_3$(**1**)] (red), *fac*-[ReBr(CO)$_3$(**2**)], the ligand based azobenzene $n \rightarrow \pi^*$ transition is also expected to overlap with the more intense ^{1}MLCT feature (see Fig. 7). The invariance in the energies of the ^{1}MLCT transitions suggests that the structural differences of the coordinated ligands (**1**–**5**) impart little influence upon the electronics of the complex in each case.

The corresponding solution state luminescence properties of the complexes *fac*-[ReBr(CO)$_3$(**1**–**5**)] showed that each species demonstrated a broad emission band peaking between 558 and 585 nm (Fig. 9, Table 1). The associated emission lifetimes of these emission bands were obtained and fell in the range of 162–269 ns.

The emission spectra also revealed a weaker feature around 450 nm, which was most pronounced for *fac*-[ReBr(CO)$_3$(**1**)]. This is tentatively attributed to residual fluorescence from the ligand which is somewhat perturbed by complexation. Firstly, these data are clearly different to the free ligand (**1**–**5**) properties, which were blue emitters with lifetimes of < 5 ns in each case. Secondly, the large Stokes' shift and relatively long emission lifetimes are consistent with an emitting state of triplet character. In accordance with previous studies, [25,31,33] we therefore attribute the emission properties of this series of complexes to a spin

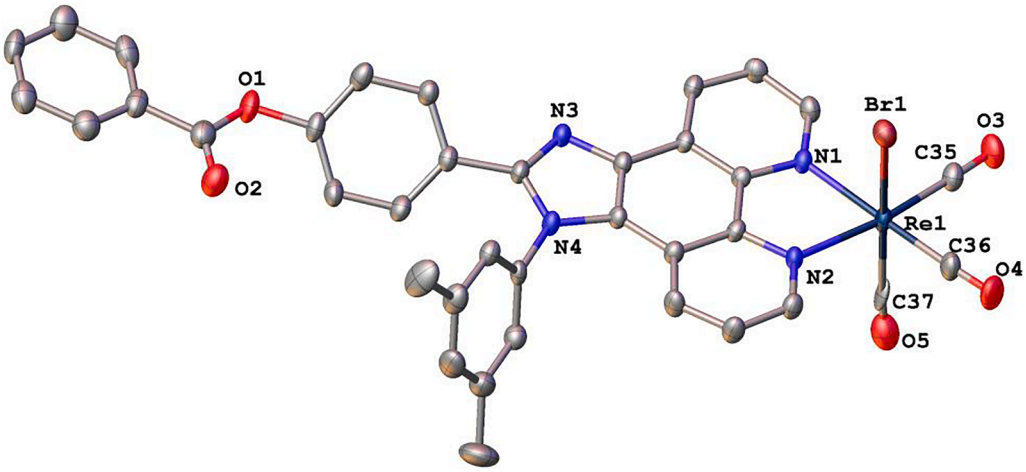

Fig. 5. X-ray structure of complex *fac*-[ReBr(CO)$_3$(**5**)]. Hydrogen atoms and toluene solvate molecules have been omitted for clarity. Selected data - bond lengths (Å): C35–Re1, 1.931(5); C36–Re1, 1.915(5); C37–Re1, 2.009(6); N1–Re1, 2.171(3); N2–Re1, 2.184(3); Br1–Re1, 2.6006(5); Bond angles (°): O3–C35–Re1, 177.8(4); O4–C36–Re1, 177.9(5); O5–C37–Re1, 174.8(5); C1–N1–Re1,125.4(3); C5–N1–Re1, 115.8(3); C12–N2–Re1, 125.8(3); C9–N2–Re1, 115.7(3); C36–Re1–C35, 87.9(2); C36–Re1–C37, 88.0(2); C35–Re1–C37, 90.30(19); C36–Re1–N1, 172.35(17); C35–Re1–N1, 96.04(17); C37–Re1–N1, 98.50(15); C36–Re1–N2, 100.81(17); C35–Re1–N2, 171.29(16); C37–Re1–N2, 90.30(19); N1–Re1–N2, 75.28(13); C36–Re1–Br1, 87.02(16); C35–Re1–Br1, 94.70(15); C37–Re1–Br1, 172.81(13); N1–Re1–Br1, 86.13(10); N2–Re1–Br1, 85.54(10). ADP ellipsoids are displayed at 50 % probability.

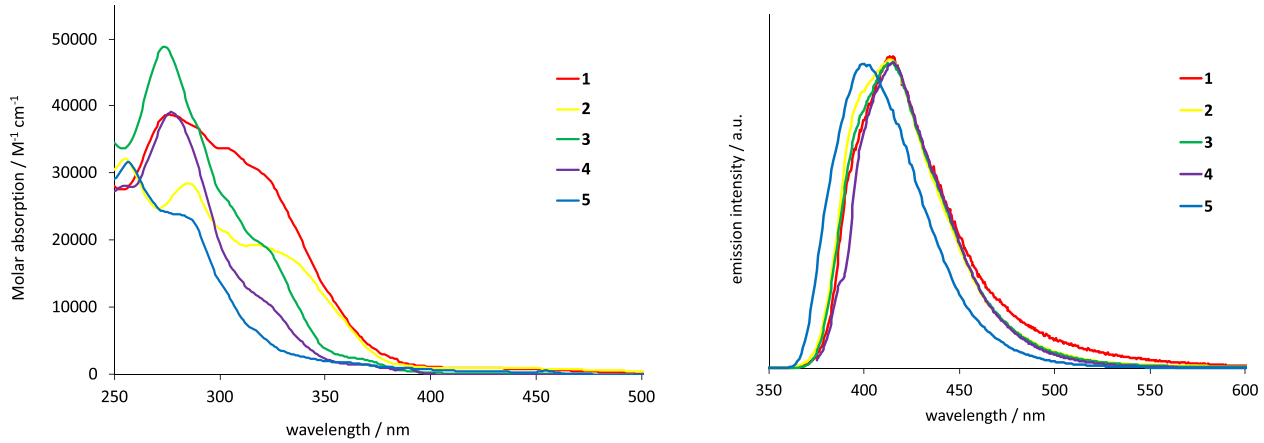

Fig. 6. A comparison of the UV–vis. absorption spectra (left), and steady state emission spectra (right, normalised) of the ligands (recorded in $CHCl_3$).

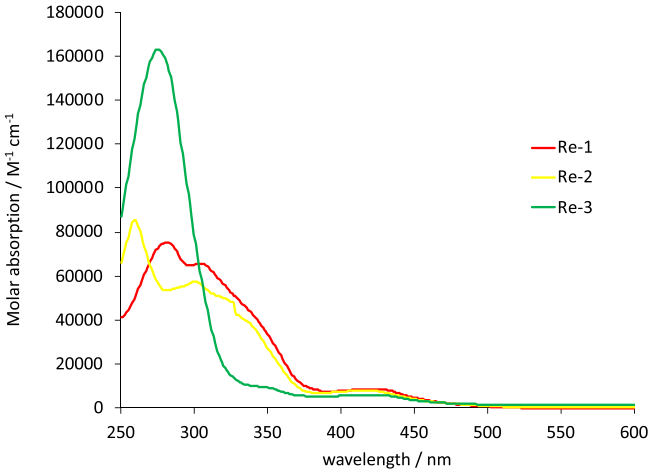

Fig. 7. A comparison of the UV–vis. absorption spectra of *fac*-[ReBr(CO)$_3$(**1**)] (red), *fac*-[ReBr(CO)$_3$(**2**)] (yellow), and *fac*-[ReBr(CO)$_3$(**3**)] (green) (recorded in $CHCl_3$). ((Colour online.))

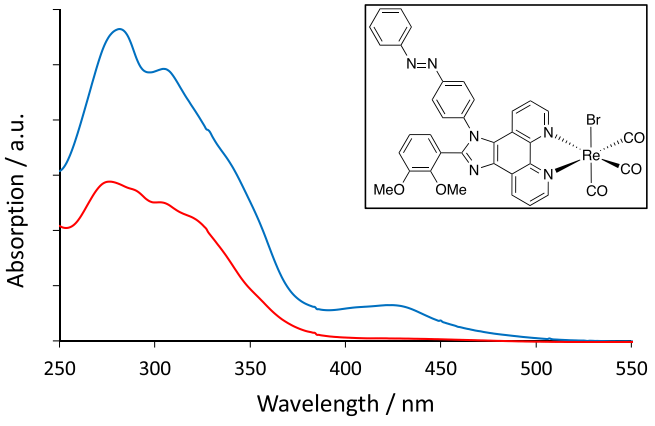

Fig. 8. A comparison of the UV–vis. absorption spectra of **2** (red) and *fac*-[ReBr(CO)$_3$(**2**)] (blue, structure shown inset). ((Colour online.))

forbidden ($T_1 \rightarrow S_0$) relaxation from a $^3M_{Re}LCT$ excited state. It is noteworthy, especially in comparison to *fac*-[ReBr(CO)$_3$(**2**)], that *fac*-[ReBr(CO)$_3$(**1**)] possesses a hypsochromically shifted emission maximum and a correspondingly longer lifetime (invoking the energy gap law) that is distinct from the other complexes in the series. While the

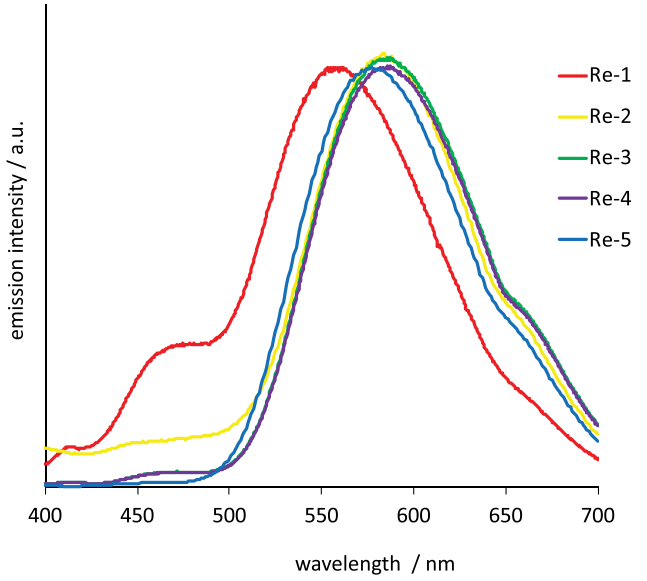

Fig. 9. Normalised emission spectral profiles (λ_{ex} = 370 nm) for the complexes *fac*-[ReBr(CO)$_3$(**1**–**5**)] recorded in aerated $CHCl_3$.

Table 1
Selected IR, UV–vis. and luminescence spectroscopic data for the Re(I) complexes.

Complex	υ(CO)/ cm^{-1} [a]	^{1}MLCT, λ_{abs}/nm (ε/M^{-1}cm^{-1}) [b]	^{3}MLCT, λ_{em}/nm[c]	^{3}MLCT, τ/ns[d]
fac-[ReBr(CO)$_3$(**1**)]	2020, 1891 br	425 (7700)	558	269
fac-[ReBr(CO)$_3$(**2**)]	2020, 1914, 1891	420 (7900)	583	197
fac-[ReBr(CO)$_3$(**3**)]	2020, 1886 br	421 (5900)	585	164
fac-[ReBr(CO)$_3$(**4**)]	2016, 1891 br	420 (8500)	585	169
fac-[ReBr(CO)$_3$(**5**)]	2019, 1890 br	422 (6300)	583	162

[a] solid state.
[b] $CHCl_3$ solution 1×10^{-5} M.
[c] λ_{ex} = 365 nm or 410 nm, aerated $CHCl_3$ solution 1×10^{-5} M.
[d] λ_{ex} = 372 nm, aerated $CHCl_3$ solution 1×10^{-5} M.

reasons for this observation are currently unclear, further investigations will consider subtle evolutions of the ligand structure to try to unravel the underpinning factors.

Finally, Fig. 10 shows the comparison of the excitation spectrum of *fac*-[ReBr(CO)$_3$(**3**)] with the absorption spectrum. The spectra show that the excitation between 350 and 450 nm, which includes both ligand-centred and the ^{1}MLCT band, is by far the most efficient means of generating the ^{3}MLCT emission. The shorter wavelength absorption feature, predominantly associated with the trityl moiety, is notably absent in the excitation profile.

6. Conclusions

In summary, a series of substituted imidazole[4,5-*f*]-1,10-phenanthroline derivatives, containing varying types of functionalised aryl substituent, including azo dye, trityl and terpyridine pendants, have been isolated and fully characterised. These ligands were demonstrated to be effective chelates for Re(I) to form complexes of the type *fac*-[ReBr(CO)$_3$(N^N). The resultant complexes were isolated as air stable powders. Two of the Re(I) complexes were structurally characterised using X-ray crystallography and showed the expected coordination sphere features as well as integrity of the functionalised ligand forms. While each of the free ligands demonstrated fluorescence in the blue region, the corresponding Re(I) complexes displayed bathochromically shifted visible emission in the range 558–585 nm which is likely due to an emitting ^{3}M$_{Re}$LCT state.

While this current work has shown the scope of functionalisation that can be introduced into imidazole[4,5-*f*]-1,10-phenanthroline type ligands, and their tolerance to coordination chemistry studies, further work will focus upon the potential uses and applications of such species. For example, the successful isolation of *fac*-[ReBr(CO)$_3$(**4**)] invites further investigation as a luminescent building block for multimetallic assemblies by employing the pendant 2,2′:6′,2′′-terpyridine unit as a secondary (and bridging) binding site. A further area of investigation could focus upon the photochromic, and photoisomerisation, behaviour of the azo dye containing species, especially if one considers the integration of the photoactive complexes into host materials. In addition, previous work has shown that a wide range of luminescent Re(I) complexes have already been successfully investigated as biologically compatible, cell imaging agents [33]. An ability to enhance the lipophilicity of such systems, as demonstrated in the current study, is important and the scope displayed here to add extremely bulky lipophilic groups such as trityl moieties could be useful in such a context.

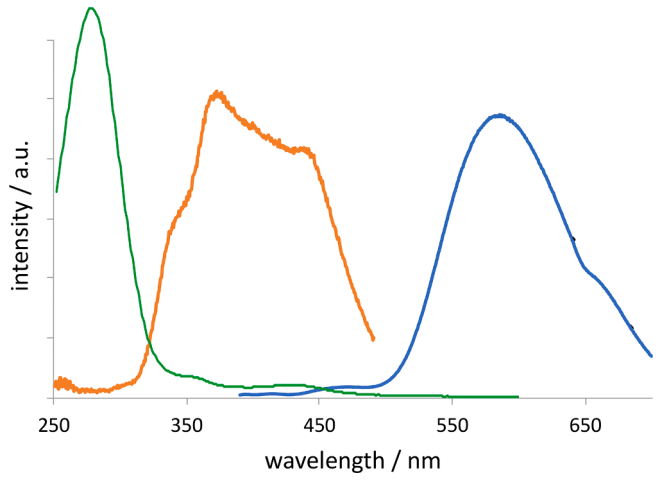

Fig. 10. A comparison of the excitation (orange) and absorption (green) spectral profiles for *fac*-[ReBr(CO)$_3$(**3**)] (emission shown in blue). ((Colour online.))

7. Experimental

All reactions were performed with the use of vacuum line and Schlenk techniques. Reagents were commercial grade and were used without further purification unless otherwise stated. [ReBr(CO)$_5$] was prepared according to the literature procedure [34]. 1,10-Phenanthroline-5,6-dione, [35] 4-(benzoyloxy)benzaldehyde [36], and 4-[2,2′:6′,2′′-terpyridin]-4′-ylbenzamine [37] were prepared as previously reported. ^{1}H and ^{13}C{^{1}H} NMR spectra were run on NMR-FT Bruker 400 or 250 spectrometers and recorded in $CDCl_3$. ^{1}H and ^{13}C{^{1}H} NMR chemical shifts (δ) were determined relative to internal TMS and are given in ppm. Low-resolution mass spectra were obtained by the staff at Cardiff University. High-resolution mass spectra were carried out by at the EPSRC National Mass Spectrometry Service at Swansea University. UV–vis studies were performed on a Jasco V-570 spectrophotometer as $CHCl_3$ solutions (10^{-5} M). Photophysical data were obtained on a JobinYvon-Horiba Fluorolog spectrometer fitted with a JY TBX picosecond photodetection module as aerated $CHCl_3$ solutions. The pulsed source was a Nano-LED configured for 295 or 372 nm output operating at 1 MHz. Luminescence lifetime profiles were obtained using the JobinYvon-Horiba FluoroHub single photon counting module and the data fits yielded the lifetime values using the provided DAS6 deconvolution software.

8. Data collection and processing

X-ray diffraction datasets were measured on a Rigaku FRE + diffractometer equipped with VHF Varimax confocal mirrors and an AFC12 goniometer and HG Saturn 724 + detector [38] using Crystal Clear software for data collection CrysAlisPro software for data reduction [39].

9. Structure analysis and refinement

The structures were solved by dual methods using SHELXT 2018/2 [40] and refined on F_o^2 by full-matrix least-squares refinements using SHELXL 2018/3 [41] within the OLEX2 suite [42]. All non-hydrogen atoms were refined with anisotropic displacement parameters, and all hydrogen atoms were added at calculated positions and refined using a riding model with isotropic displacement parameters based on the equivalent isotropic displacement parameter (U_{eq}) of the parent atom. Geometric and thermal restraints were applied to disorder components to model appropriately atomic displacement parameters.

10. Synthesis of ligand 1

Into a round bottom flask was added 4-*tert*-butylbenzaldehyde (0.24 ml, 1.43 mmol), 1,10-phenanthroline-5,6-dione (0.300 g, 1.43 mmol), 4-phenylazoaniline (0.282 g, 1.43 mmol), ammonium acetate (1.10 g, 14.3 mmol) and acetic acid (30 ml). The reaction mixture was heated to reflux for 3 h and then, upon cooling, a product was precipitated from water (50 ml). The light brown precipitate was extracted with chloroform (2 × 150 ml). The combined organic phases were washed with water (3 × 50 ml) and brine (1 × 50 ml), then dried and the volatiles removed *in vacuo*. The crude product was recrystalised from chloroform and hexane to give product **1** as an orange powder (0.360 g, 47 %). ^{1}H NMR (400 MHz, $CDCl_3$) δ 9.22 (1H, d, J = 4.2 Hz), 9.18 (1H, d, J = 8.1 Hz), 9.06 (1H, d, J = 3.3 Hz), 8.19 (2H, d, J = 8.4 Hz), 8.05 – 7.99 (2H, m), 7.82 – 7.76 (1H, m), 7.71 (2H, d, J = 8.4 Hz), 7.60 – 7.51 (6H, m), 7.38 – 7.29 (3H, m), 1.27 (9H, s, CH_3) ppm. ^{13}C{^{1}H} NMR (101 MHz, $CDCl_3$) δ 153.1, 152.8, 152.4, 152.4, 149.1, 148.0, 144.9, 144.4, 139.9, 136.4, 132.1, 130.7, 129.8, 129.4, 129.1, 128.0, 126.8, 125.6, 124.8, 124.0, 123.6, 123.3, 122.3, 119.8, 34.8, 31.2 ppm. HRMS (EI)(%): found m/z = 533.2441; $[C_{35}H_{29}N_6]^+$ requires 533.2448. IR (KBr plates): 2963 (w), 1594 (w), 1556 (w), 1502 (m), 1471 (w), 1442 (m), 1376 (w), 1339 (w), 1300 (w), 1268 (w), 1152 (w), 1062 (w), 1018 (w), 977 (w), 867

(w), 841 (s), 809 (m), 795 (w), 769 (s) cm^{-1}. UV–vis λ^{max} (ε/M^{-1} cm^{-1}) ($CHCl_3$): 280 (39000), 305 sh (33500), 430 sh (800) nm.

11. Synthesis of ligand 2

This material was prepared as for **1** but using 2,3-dimethoxybenzaldehyde (0.237 g, 1.43 mmol), 1,10-phenanthroline-5,6-dione (0.300 g, 1.43 mmol), 4-phenylazoaniline (0.282 g, 1.43 mmol), and ammonium acetate (1.10 g, 14.3 mmol). The crude product was recrystalised from chloroform and hexane to give product **2** as an orange powder (0.490 g, 64 %). ^{1}H NMR (400 MHz, $CDCl_3$) δ 9.25 (1H, dd, J = 4.4, 1.5 Hz), 9.17 (1H, dd, J = 8.1, 1.5 Hz), 9.10 (1H, dd, J = 4.3, 1.3 Hz), 8.03 (2H, d, J = 8.4 Hz), 7.95 (2H, dd, J = 7.5, 1.8 Hz), 7.79 (1H, dd, J = 8.1, 4.5 Hz), 7.67 (1H, dd, J = 8.4, 1.3 Hz), 7.62 (2H, d, J = 8.4 Hz), 7.58 – 7.51 (3H, m), 7.36 (1H, dd, J = 8.4, 4.4 Hz), 7.09 – 6.94 (3H, m), 3.83 (3H, s, CH_3), 3.78 (3H, s, CH_3) ppm. ^{13}C{^{1}H} NMR (101 MHz, $CDCl_3$) δ 153.0, 153.0, 152.8, 151.1, 149.4, 148.6, 148.4, 145.2, 144.7, 139.4, 136.5, 132.2, 131.0, 129.7, 129.5, 128.7, 126.6, 125.4, 124.5, 124.5, 124.5, 124.0, 123.7, 123.5, 122.7, 120.1, 114.7, 62.0, 56.3 ppm. HRMS (EI)(%): found m/z = 536.1962; $[C_{33}H_{24}N_6O_2]^+$ requires 536.1955. IR (KBr plates): 2931 (w), 2828 (w), 1597 (w), 1579 (w), 1559 (m), 1505 (m), 1476 (s), 1461 (m), 1426 (m), 1381 (m), 1340 (w), 1328 (w), 1303 (w), 1263 (s), 1235 (w), 1158 (w), 1081 (s), 1074 (m), 1055 (w), 990 (s), 928 (w), 874 (w), 816 (w) cm^{-1}. UV–vis λ^{max} (ε/M^{-1} cm^{-1}) ($CHCl_3$): 255 (32000), 289 (27500), 319 sh (19800), 417 sh (650) nm.

12. Synthesis of ligand 3

This material was prepared by a similar method to **1** using 4-*tert*-butylbenzaldehyde (0.24 ml, 1.43 mmol), 1,10-phenanthroline-5,6-dione (0.300 g, 1.43 mmol), 4-tritylaniline (0.480 g, 1.43 mmol), and ammonium acetate (1.10 g, 14.3 mmol). The crude product was recrystalised from acetone to give product **3** as an off-white powder (0.200 g, 21 %). ^{1}H NMR (400 MHz, $CDCl_3$) δ 9.18 (1H, dd, J = 4.3, 1.6 Hz), 9.14 (1H, dd, J = 8.1, 1.6 Hz), 9.07 (1H, dd, J = 4.3, 1.6 Hz), 7.75 (1H, dd, J = 8.1, 4.4 Hz), 7.53 (5H, d, J = 5.3 Hz), 7.43 (2H, d, J = 8.6 Hz), 7.38 – 7.27 (18H, m), 1.35 (9H, s, CH_3) ppm. ^{13}C{^{1}H} NMR (101 MHz, $CDCl_3$) δ 152.7, 152.4, 149.7, 149.1, 147.9, 146.2, 144.9, 144.4, 136.2, 135.9, 133.3, 131.2, 130.6, 129.0, 128.0, 128.0, 127.0, 126.9, 126.6, 125.4, 124.1, 123.6, 122.1, 119.9, 65.2, 34.9, 31.3 ppm. HRMS (EI)(%): found m/z = 671.3167; $[C_{48}H_{39}N_4]^+$ requires 671.3169. IR (KBr plates): 3055 (w), 2957 (w), 1598 (w), 1558 (w), 1506 (m), 1492 (s), 1468 (w), 1443 (s), 1391 (w), 1340 (w), 1299 (w), 1191 (w), 1152 (w), 1035 (w), 980 (w), 841 (s), 808 (w), 767 (w), 753 (s), 741 (s), 701 (s) cm^{-1}. UV–vis λ^{max} (ε/M^{-1} cm $^{-1}$) ($CHCl_3$): 276 (48600), 300 sh (25900), 321 sh (19400), 362 sh (2500) nm.

13. Synthesis of ligand 4

This material was prepared by a similar method to **1** using 4-*tert*-butylbenzaldehyde (0.15 ml, 0.892 mmol), 1,10-phenanthroline-5,6-dione (0.187 g, 0.892 mmol), 4-[2,2′:6′,2′′-terpyridin]-4′-ylbenzamine (0.230 g, 0.981 mmol), and ammonium acetate (0.688 g, 8.92 mmol). The crude product was recrystalised from chloroform/hexane and the filtered through a pad of silica in 2 % methanol in chloroform to give product **4** as an off-white powder (0.110 g, 19 %). ^{1}H NMR (400 MHz, $CDCl_3$) δ 9.21 (1H, dd, J = 4.4, 1.8 Hz), 9.18 (1H, dd, J = 8.1, 1.8 Hz), 9.08 (1H, dd, J = 4.3, 1.6 Hz), 8.86 (2H, s), 8.78 – 8.75 (2H, m), 8.73 (2H, d, J = 7.9 Hz), 8.15 (2H, d, J = 8.4 Hz), 7.94 (2H, td, J = 7.7, 1.8 Hz), 7.78 (1H, dd, J = 8.1, 4.4 Hz), 7.73 – 7.69 (2H, m), 7.59 – 7.54 (3H, m), 7.45 – 7.36 (5H, m), 1.31 (9H, s, CH_3) ppm. ^{13}C{^{1}H} NMR (101 MHz, $CDCl_3$) δ 156.5, 156.0, 152.9, 152.6, 149.4, 149.1, 148.1, 140.9, 138.8, 137.4, 136.4, 130.9, 130.1, 129.7, 129.6, 129.1, 128.1, 127.0, 126.9, 125.8, 125.6, 124.4, 124.2, 123.7, 122.6, 121.7, 120.0, 119.3, 35.0, 31.3 ppm. HRMS (ES)(%): found m/z = 660.2868; $[C_{42}H_{34}N_7]^+$ requires 660.2870. IR: 2954 (w), 1608 (w), 1585 (m), 1568 (m), 1516 (m), 1467 (m), 1444 (m), 1390 (m), 1265 (w), 1114 (w), 842 (m), 790 (s) cm^{-1}. UV–vis λ^{max} (ε/M^{-1} cm^{-1}) ($CHCl_3$): 277 (38700), 321 sh (10900), 366 sh (1800) nm.

14. Synthesis of ligand 5

This material was prepared by a similar method to **1** using 4-(benzoyloxy)benzaldehyde (0.324 g, 1.43 mmol), 1,10-phenanthroline-5,6-dione (0.300 g, 1.43 mmol), 3,5-dimethylaniline (0.18 ml, 1.43 mmol), and ammonium acetate (1.10 g, 14.3 mmol). The crude product was recrystalised from chloroform and hexane to give product **5** as an off-white powder (0.400 g, 55 %). ^{1}H NMR (400 MHz, $CDCl_3$) δ 9.19 (1H, dd, J = 4.4, 1.7 Hz), 9.14 (1H, dd, J = 8.1, 1.8 Hz), 9.05 (1H, dd, J = 4.3, 1.6 Hz), 8.22 – 8.15 (2H, m), 7.79 – 7.71 (3H, m), 7.67 – 7.60 (1H, m), 7.51 (2H, app. t, J = 7.7 Hz), 7.45 (1H, dd, J = 8.4, 1.6 Hz), 7.35 – 7.29 (2H, m), 7.24 – 7.18 (2H, m), 7.16 (2H, s), 2.43 (6H, s, CH_3) ppm. ^{13}C{^{1}H} NMR (101 MHz, $CDCl_3$) δ 164.9 (C=O), 151.7, 151.1, 149.1, 148.0, 145.0, 144.5, 140.8, 137.8, 136.1, 133.9, 132.2, 130.6, 130.4, 130.3, 129.3, 128.7, 128.3, 127.8, 127.2, 126.2, 124.0, 123.6, 122.3, 121.8, 120.0, 21.5 ppm. IR (KBr plate): 2928 (m), 1734 (s), 1609 (w), 1599 (w), 1565 (w), 1471 (s), 1450 (s), 1393 (w), 1342 (w), 1333 (w), 1263 (s), 1202 (s), 1166 (m), 1078 (s), 1061 (s), 880 (w) cm^{-1}. UV–vis λ^{max} (ε/M^{-1} cm^{-1}) ($CHCl_3$): 258 (31700), 286 (23800), 319 sh (6200) nm.

15. Synthesis of *fac*-[ReBr(CO)$_3$(1)]

Into a round bottom flask was added ligand **1** (0.066 g, 0.123 mmol), pentacarbonylbromorhenium (0.05 g, 0.123 mmol) and toluene (30 ml) and the reactants were left at reflux for 3 h. The solvent was removed *in vacuo* to yield orange oil. $CHCl_3$ was added (2 ml) and was precipitated from hexane to give product. The title compound was prepared to give the product *fac*-[ReBr(CO)$_3$(**1**)] as a yellow/orange solid (0.085 g, 78 %). ^{1}H NMR (400 MHz, $CDCl_3$) δ 9.62 (1H, br s), 9.42 (1H, d, J = 4.7 Hz), 9.31 (1H, d, J = 5.2 Hz), 8.27 (2H, d, J = 8.1 Hz), 8.08 – 8.02 (2H, m), 8.02 – 7.95 (1H, m), 7.80 – 7.72 (2H, m), 7.69 – 7.52 (6H, m), 7.41 (2H, d, J = 8.2 Hz), 7.17 (1H, d, J = 7.9 Hz), 1.30 (9H, s, CH_3) ppm. ^{13}C{^{1}H} NMR (101 MHz, $CDCl_3$) δ 197.0 (C=O), 189.1 (C=O), 154.5, 153.9, 153.6, 152.4, 151.9, 150.8, 145.5, 145.1, 138.8, 137.1, 133.1, 132.5, 130.0, 129.7, 129.5, 129.2, 128.4, 127.3, 126.4, 126.2, 126.0, 125.4, 125.2, 125.0, 123.4, 122.1, 35.0, 31.2 ppm. HRMS (EI)(%): found m/z = 905.0829; $[C_{38}H_{28}BrN_6O_3^{185}Re + Na]^+$ requires 905.0828. IR (KBr plate): 2960 (w), 2020 (s), 1891 (b), 1600 (w), 1500 (w), 1473 (w), 1447 (m), 1380 (w), 1303 (w), 1267 (w), 1155 (w), 1121 (w), 1017 (w), 988 (w), 841 (w), 805 (w), 770 (w), 724 (w) cm^{-1}. UV–vis λ^{max} (ε/M^{-1} cm^{-1}) ($CHCl_3$): 282 (74700), 306 (62500), 425 (7700) nm.

16. Synthesis of *fac*-[ReBr(CO)$_3$(2)]

As for *fac*-[ReBr(CO)$_3$(**1**)], but using ligand **2** (0.066 g, 0.123 mmol), pentacarbonylbromorhenium (0.05 g, 0.123 mmol) and toluene (30 ml) to give product *fac*-[ReBr(CO)$_3$(**2**)] as an orange powder (0.072 g, 66 %). ^{1}H NMR (400 MHz, $CDCl_3$) δ 9.34 (1H, dd, J = 5.1, 1.3 Hz), 9.30 (1H, dd, J = 8.3, 1.2 Hz), 9.24 (1H, dd, J = 5.1, 1.2 Hz), 8.04 – 7.96 (2H, m), 7.92 – 7.86 (3H, m), 7.77 (1H, dd, J = 8.6, 1.2 Hz), 7.61 – 7.52 (2H, m), 7.52 – 7.44 (4H, m), 7.05 – 7.00 (1H, m), 6.96 – 6.91 (2H, m), 3.77 (3H, s, CH_3), 3.71 (3H, s, CH_3) ppm. ^{13}C {^{1}H} NMR (101 MHz, $CDCl_3$) δ 197.0 (C=O), 189.1 (C=O), 153.2, 153.1, 152.8, 152.4, 151.8, 151.1, 148.0, 145.6, 145.1, 137.9, 136.8, 132.9, 132.2, 130.3, 129.5, 129.2, 128.9, 126.8, 126.6, 126.2, 125.1, 124.6, 124.5, 124.5, 124.1, 123.3, 123.0, 122.0, 115.0, 61.7, 56.0 ppm. HRMS (ES)(%): found m/z = 885.0593; $[C_{36}H_{25}BrN_6O_5^{185}Re]^+$ requires 885.0594. IR (KBr plates): 2020 (s), 1914 (s), 1891 (s),1710 (m), 1616 (w), 159 (w), 1581 (w), 1530 (w), 1501 (w), 1478 (w), 1458 (w), 1384 (w), 1362 (w), 1302 (w), 1266 (w), 1221 (w), 1086 (w), 1062 (w), 993 (w) cm^{-1}. UV–vis λ^{max} (ε/M^{-1} cm^{-1}) ($CHCl_3$): 260 (84400), 301 (55100), 330 (sh) (35000),

420 (7900) nm.

17. Synthesis of *fac*-[ReBr(CO)$_3$(3)]

As for *fac*-[ReBr(CO)$_3$(**1**)], but using ligand **3** (0.058 g, 0.123 mmol), pentacarbonylbromorhenium (0.05 g, 0.123 mmol) and toluene (30 ml) to give product *fac*-[ReBr(CO)$_3$(**3**)] as a yellow/orange powder (0.040 g, 32 %). ^{1}H NMR (400 MHz, CDCl$_3$) δ 9.40 – 9.37 (1H, m), 9.34 (1H, dd, J = 8.3, 1.4 Hz), 9.27 (1H, dd, J = 5.1, 1.3 Hz), 7.94 (1H, dd, J = 8.3, 5.1 Hz), 7.66 – 7.59 (3H, m), 7.59 – 7.54 (2H, m), 7.49 – 7.41 (3H, m), 7.41 – 7.27 (17H, m), 1.36 (9H, s, CH_3) ppm. ^{13}C{^{1}H} NMR (101 MHz, CDCl$_3$) δ 151.8, 150.7, 146.0, 145.5, 142.3, 136.9, 135.0, 133.9, 133.7, 133.0, 131.1, 129.9, 129.1, 128.1, 127.9, 127.6, 126.7, 126.4, 126.1, 126.1, 125.7, 124.8, 122.1, 65.3, 35.0, 31.3 ppm. MS (ES)(%): found m/z = 1021.12; [C$_{51}$H$_{38}$BrN$_4$O$_3$Re + H]$^+$ requires 1021.17. IR (KBr plates): 2955 (w), 2020 (s), 1886 (bs), 1600 (w), 1447 (w), 842 (w), 806 (w), 753 (w), 723 (w), 700 (w) cm^{-1}. UV–vis λ^{max} (ε/M^{-1} cm $^{-1}$) (CHCl$_3$): 276 (16800), 346 sh (12400), 421 (5900) nm.

18. Synthesis of *fac*-[ReBr(CO)$_3$(4)]

As for *fac*-[ReBr(CO)$_3$(**1**)], but using ligand **4** (0.050 g, 0.076 mmol), pentacarbonylbromorhenium (0.030 g, 0.076 mmol) and toluene (30 ml) to give product *fac*-[ReBr(CO)$_3$(**4**)] as orange powder (0.050 g, 63 %).^{1}H NMR (400 MHz, d6-DMSO) δ 9.46 (1H, dd, J = 5.1, 1.2 Hz), 9.40 (1H, dd, J = 8.3, 1.3 Hz), 9.32 (1H, d, J = 4.1 Hz), 8.88 (2H, s), 8.77 (2H, d, J = 4.6 Hz), 8.71 (1H, d, J = 8.0 Hz), 8.33 (1H, d, J = 8.7 Hz), 8.22 (1H, dd, J = 8.2, 5.2 Hz), 8.11 – 7.98 (4H, m), 7.90 – 7.84 (2H, m), 7.75 (1H, d, J = 7.6 Hz), 7.68 – 7.63 (3H, m), 7.55 (2H, dd, J = 6.5, 4.8 Hz), 7.48 – 7.43 (2H, m), 1.25 (9H, s, CH_3) ppm. Insufficient solubility to obtain ^{13}C{^{1}H} NMR. MS (ES)(%): found m/z = 1010.14; [C$_{47}$H$_{33}$BrN$_7$O$_3$Re + H]$^+$ requires 1010.14. IR (KBr plates): 2965 (w), 2016 (s), 1891 (s), 1600 (w), 1582 (w), 1516 (w), 1466 (w), 1384 (w), 792 (w), 760 (w), 722 (w) cm^{-1}. UV–vis λ^{max} (ε/M^{-1} cm $^{-1}$) (CHCl$_3$): 278 (94 000), 338 (sh) (16 900), 420 (8500) nm.

19. Synthesis of *fac*-[ReBr(CO)$_3$(5)]

As for *fac*-[ReBr(CO)$_3$(**1**)], but using ligand **5** (0.064 g, 0.123 mmol) and pentacarbonylbromorhenium (0.05 g, 0.123 mmol) to give the product *fac*-[ReBr(CO)$_3$(**5**)] as a yellow/orange powder (0.085 g, 78 %). ^{1}H NMR (400 MHz, CDCl$_3$) δ 9.39 (1H, dd, J = 5.1, 1.4 Hz), 9.35 (1H, dd, J = 8.3, 1.4 Hz), 9.27 (1H, dd, J = 5.0, 1.4 Hz), 8.22 – 8.18 (2H, m), 7.95 (1H, dd, J = 8.2, 5.1 Hz), 7.79 – 7.75 (2H, m), 7.69 – 7.64 (1H, m), 7.60 (1H, dd, J = 8.6, 1.4 Hz), 7.56 – 7.50 (3H, m), 7.39 (1H, s), 7.28 – 7.24 (2H, m), 7.21 – 7.17 (2H, m), 2.50 (3H, s, CH_3), 2.48 (3H, s, CH_3) ppm. ^{13}C{^{1}H} NMR (101 MHz, CDCl$_3$) δ 197.1 (C≡O), 197.0 (C≡O), 189.1 (C≡O), 164.9 (C═O), 153.2, 152.4, 151.8, 150.8, 145.5, 145.2, 141.7, 141.5, 136.9, 136.7, 134.1, 133.0, 133.0, 130.6, 130.4, 130.3, 129.2, 128.8, 127.6, 126.9, 126.4, 126.1, 126.0, 125.7, 125.0, 122.3, 122.2, 21.5 ppm. MS (ES)(%): found m/z = 893.05; [C$_{36}$H$_{25}$BrN$_6$O$_5$Re + Na]$^+$ requires 893.05. IR (KBr plates): 3063 (w), 2019 (s), 1890 (bs), 1735 (s), 1711 (s), 1600 (m), 1510 (w), 1469 (m), 1450 (m), 1361 (w), 1262 (s), 1207 (s), 1168 (s), 1059 (s), 1023 (m), 808 (m), 739 (w), 707 (s) cm^{-1}. UV–vis λ^{max} (ε/M^{-1} cm $^{-1}$) (CHCl$_3$): 277 (67000), 299 (sh) (43800), 336 (sh) (14400), 422 (6300) nm.

Declaration of Competing Interest

The authors declare that they have no known competing financial interests or personal relationships that could have appeared to influence the work reported in this paper.

Data availability

Data will be made available on request.

Acknowledgements

(Knowledge Economy Skills Scholarship to ROB) and Magnox Ltd are thanked for financial support. We thank the staff of the EPSRC Mass Spectrometry National Service (Swansea University) and the UK National Crystallographic Service at the University of Southampton.

Appendix A. Supplementary data

Supplementary data to this article can be found online at https://doi.org/10.1016/j.poly.2022.116179.

References

[1] D. Yanover, M. Kaftory, Acta Cryst. C C65 (2009), o365.
[2] (a) E.H. White, M.J.C. Harding, J. Am. Chem. Soc. 86 (1964) 5686;
(b) K. Maeda, H. Ojima, T. Hayashi, Bull. Chem. Soc. Jap. 38 (1965) 76.
[3] K. Nakashima, Y. Fukuzaki, R. Nomura, R. Shimoda, Y. Nakamura, N. Kuroda, S. Akiyama, K. Irgum, Dyes Pigments 38 (1998) 127.
[4] (a) K. Yagi, C.F. Soong, M. Irie, J. Org. Chem. 66 (2001) 5419;
(b) Y.-X. Peng, N. Wang, Y. Dai, B. Hu, B.B. Ma, W. Huang, RSC Adv. 5 (2015) 6395;
(c) A. Patel, S.Y. Sharp, K. Hall, W. Lewis, M.F.G. Stevens, P. Workman, C. J. Moody, Org. Biomol. Chem. 1 (2016) 3889.
[5] K. Feng, F.L. Hsu, D. Van DerVeer, K. Bota, X.R. Bu, J. Photochem. Photobiol. A 165 (2004) 223.
[6] T. Cardinaels, J. Ramaekers, P. Nockermann, K. Driesen, K. Van Hecke, L. Van Meervelt, S. Lei, S. De Feyter, D. Guillon, B. Donnio, K. Binnemans, Chem. Mater. 20 (2008) 1278.
[7] (a) L. Li, J.-Q. Cao, H.-M. Liu, Q. Wu, Q.-H. Pan, Z.-P. Zeng, Y.-T. Lan, Y.-M. Li, W.-J. Mei, X.-C. Wang, W.-J. Zheng, Molecules 22 (2017) 829;
(b) P. Gratal, M.-S. Arias-Perez, L. Gude, Bioorg. Chem. (2022), https://doi.org/10.1016/j.bioorg.2022.105851.
[8] (a) C. Reichardt, T. Sainuddin, M. Wachtler, S. Monro, S. Kupfer, J. Guthmuller, S. Grafe, S. McFarland, B. Dietzek, J. Phys. Chem. A 120 (2016) 6379;
(b) H.-Q. Zheng, Y.-P. Guo, M.-C. Yin, Y.-T. Fan, Chem. Phys. Lett. 653 (2016) 17;
(c) Z.-Z. Lu, J.-D. Peng, A.-K. Wu, C.-H. Lin, C.-G. Wu, K.-C. Ho, Y.-C. Lin, K.-L. Lu, Eur. J. Inorg. Chem. (2016) 1214;
(d) B.N. Bideh, C. Roldan-Carmona, H. Shahroosvand, M.K. Nazeeruddin, Dalton Trans. 45 (2016) 7195;
(e) A.R. Santos, D. Escudero, L. Gonzalez, G. Orellana, Chem. Asian J. 10 (2015) 622.
[9] L. Martins, L.K. Macreadie, D. Sensharma, S. Vaesen, X. Zhang, J.J. Gough, M. O'Doherty, N.-Y. Zhu, M. Ruther, J.E. O'Brien, A.L. Bradley, W. Schmitt, Chem. Commun. 55 (2019) 5013.
[10] (a) J.-W. Zhu, S.-H. Liu, G.-Q. Zhang, H.-H. Xu, Y.-X. Wang, Y. Wu, Y.-M. Liu, Y. Wang, J.-B. Liang, Q.-F. Guo, J. Mem. Biol. 249 (2016) 483;
(b) S. Nikolic, L. Rangasamy, N. Gligorijevic, S. Arandelovic, S. Radulovic, G. Gasser, S. Grguric-Sipka, J. Inorg. Biochem. 160 (2016) 156;
(c) R.R. Mallepally, V.R. Putta, N. Chintakuntla, R.K. Vuradi, L.R. Kotha, S. Sirasani, J. Fluoresc. 26 (2016) 1101;
(d) L.M. Chen, F. Peng, G.D. Li, X.M. Jie, K.R. Cai, C. Cai, Y. Zhong, H. Zeng, W. Li, Z. Zhang, J. Inorg. Biochem. 156 (2016) 64;
(e) C. Qian, J.-H. Wu, L.-N. Ji, H. Chao, Dalton Trans. 45 (2016) 10546;
(f) J.-J. Li, X.-C. Hu, S. Shi, Y.-W. Zhang, T.-M. Yao, J. Mat. Chem. B 4 (2016) 1361;
(g) L.-L. Chen, H. Chao, Q.-W. Zhao, H. Li, Inorg. Chem. 54 (2015) 8281;
(h) G.L. Liao, X. Chen, J.-H. Wu, C. Qian, Y. Wang, L.-N. Ji, H. Chao, Dalton Trans. 44 (2015) 15145;
(i) T. Nandhini, K.R. Anju, V.M. Manikanamathavan, V.G. Vaidyanathan, B. U. Nair, Dalton Trans. 44 (2015) 9044;
(j) Z.-B. Zheng, S.-Y. Kang, X. Yi, N. Zhang, K.-Z. Wang, J. Inorg. Biochem. 141 (2014) 70;
(k) X.-J. He, L.-F. Tan, Inorg. Chem. 53 (2014) 11152;
(l) K. Adamson, C. Dolan, N. Moran, R.J. Forster, T.E. Keyes, Bioconj. Chem. 25 (2014) 928;
(m) A. Srishailam, Y.P. Kumar, P.V. Reddy, N. Nambigari, U. Vuruputuri, S. S. Singh, S. Satyanarayana, J. Photochem. Photobiol. B 132 (2014) 111;
(n) S. Maji, B. Sarkar, M. Patra, A.K. Da, S.M. Mobin, W. Kaim, G.K. Lahiri, Inorg. Chem. 47 (2008) 3218;
(o) M. Stephenson, C. Reichardt, M. Pinto, M. Wachtler, T. Sainuddin, G. Shi, H. Yin, S. Monro, E. Sampson, B. Dietzek, S.A. McFarland, J. Phys. Chem. A. 118 (2014) 10507.
[11] B. Yu, T.W. Rees, J. Liang, C. Jin, Y. Chen, L. Ji, H. Chao, Dalton Trans. 48 (2019) 3914.
[12] G.-B. Jiang, W.-Y. Zhang, M. He, Y.-Y. Gu, L. Bai, Y.-J. Wang, Q.-Y. Yi, F. Du, Polyhedron 169 (2019) 209.
[13] Z.-Y. Liu, J. Zhang, Y.-M. Sun, C.-F. Zhu, Y.-N. Lu, J.-Z. Wu, J. Li, H.-Y. Liu, Y. Ye, J. Mat. Chem. B 8 (2020) 438.
[14] J. Liu, Y. Chen, G. Li, P. Zhang, C. Jin, L. Zeng, L. Ji, H. Chao, Biomaterials 56 (2015) 140.

[15] (a) D. Tordera, A. Pertegas, N.M. Shavaleev, R. Scopelliti, E. Orti, H.J. Bolink, E. Baranoff, M. Gratzel, M.K. Nazeeruddin, J. Mater. Chem. 22 (2012) 19264;
(b) J.-Q. Wang, X.-J. Hou, Z.-Z. Zhao, H.-B. Bo, Q.-Z. Chen, Inorg. Chem. Commun. 67 (2016) 40;
(c) C.-Z. Jin, J.-P. Liu, Y. Chen, G.-Y. Li, R.-L. Guan, P.-Y. Zhang, L.-N. Ji, H. Chao, Dalton Trans. 44 (2015) 7538;
(d) Y. Chen, W.-C. Xu, J.-R. Zuo, L.-N. Ji, H. Chao, J. Mat. Chem. B 3 (2015) 3306;
(e) C. Dolan, R.D. Moriarty, E. Lestini, M. Devocelle, R.J. Forster, T.E. Keyes, J. Inorg. Biochem. 119 (2013) 65;
(f) D.P.E. Dayanidhi, R.P. Malapati, V.V. Ganesan, Dalton Trans. 48 (2019) 13536;
(g) A.R. Rubio, J. Fidalgo, J. Martin-Vargas, C. Perez-Arnaiz, S.R. Alonso-Torre, T. Biver, G. Espino, N. Busto, B. Barcia, J. Inorg. Biochem. 203 (2020);
(h) D.D.P. Elisa, V.V. Ganesan, J. Biol. Inorg. Chem. (2020), https://doi.org/10.1007/s00775-020-01762-7;
(i) E.E. Langdon-Jones, B.D. Ward, S.J.A. Pope, J. Organometal. Chem. 861 (2019) 234;
(j) D.D.P. Elisa, R.P. Malati, V.V. Ganesan, Dalton Trans. 48 (2019) 13536.

[16] (a) N.M. Shavaleev, H. Adams, J.A. Weinstein, Inorg. Chim. Acta 360 (2007) 700;
(b) B. Coban, I.O. Tekin, A. Sengul, U. Yildiz, I. Kocak, N. Sevinc, J. Biol. Inorg. Chem. 21 (2016) 163;
(c) X.-J. Luo, Q.-P. Qin, Y.-L. Li, Y.-C. Liu, Z.-F. Chen, H. Laing, Inorg. Chem. Commun. 46 (2014) 176.

[17] (a) R. Liu, M.-M. Huang, X.-X. Yao, H.-H. Li, F.-L. Yang, X.-L. Li, Inorg. Chim. Acta 434 (2015) 172;
(b) S.-X. Xu, J.-L. Wang, F. Zhao, H.-Y. Xia, Y.-B. Wang, Trans. Met. Chem. 40 (2015) 723;
(c) Y. Shi, X. Liu, Y. Shan, X. Zhang, W. Kong, Y. Lu, Z. Tan, X.-L. Li, Dalton Trans. 48 (2019) 2430;
(d) M.-A. Schmid, M. Rentschler, W. Frey, S. Tschierlei, M. Karnahl, Inorganics 6 (2018) 134.

[18] X. Wang, W. Zheng, H. Lin, G. Liu, Y. Chen, J. Fang, Tet. Lett. 50 (2009) 1536.

[19] X. Yi, C. Zhang, S. Guo, J. Ma, J. Zhao, Dalton Trans. 43 (2014) 1672.

[20] C. Jin, J. Liu, Y. Chen, L. Zeng, R. Guan, C. Ouyang, L. Ji, H. Chao, Chem. Eur. J. 21 (2015) 12000.

[21] J. Liu, C. Jin, B. Yuan, X. Liu, Y. Chen, L. Ji, H. Chao, Chem. Commun. 53 (2017) 2052.

[22] C. Jin, J. Liu, Y. Chen, R. Guan, C. Ouyang, Y. Zhu, L. Ji, H. Chao, Sci. Rep. 6 (2016) 22039.

[23] (a) S. Song, X. Li, Y.-H. Zhang, R. Huo, D. Ma, Dalton Trans. 43 (2014) 5974;
(b) R. An, X.-F. Wang, H.-M. Hu, Z. Zhang, C. Bai, G.-L. Xue, CrystEngComm 17 (2015) 8298;
(c) B. Xu, Q. Chen, H.-M. Hu, R. An, X.-F. Wang, G.-L. Xue, Cryst. Growth Des. 15 (2015) 2318;
(d) S. Ren, W. Jiang, Q. Wang, Z. Li, Y. Qiao, G. Che, RSC Adv. 9 (2019) 3102.

[24] Q. Yang, X. Cheng, Y.X. Wang, B.W. Wang, Z.M. Wang, S. Gao, Dalton Trans. 44 (2015) 8938.

[25] (a) R.O. Bonello, I.R. Morgan, B.R. Yeo, L.E.J. Jones, B.M. Kariuki, I.A. Fallis, S.J. A. Pope, J. Organometal. Chem. 749 (2014) 150;
(b) R.O. Bonello, M.B. Pitak, S.J. Coles, A.J. Hallett, I.A. Fallis, S.J.A. Pope, J. Organometal. Chem. 841 (2017) 39.

[26] J.-X. Wang, H.-Y. Xia, W.-Q. Liu, F. Zhao, Y.-B. Wang, Inorg. Chim. Acta 394 (2013) 92.

[27] H.-Q. Liu, Y.-X. Peng, Y. Zhang, X.-Q. Yang, F.-D. Feng, X.-B. Luo, L.-S. Yan, B. Hu, W. Huang, Dyes and Pigments 174 (2020), 108074.

[28] S. Li, C. Zhang, S. Huang, F. Hu, J. Yin, S.H. Liu, RSC Adv. 2 (2012) 4215.

[29] (a) T. Klemens, A. Świtlicka-Olszewska, B. Machura, M. Grucela, E. Schab-Balcerzak, K. Smolarek, S. Mackowski, A. Szlapa, S. Kula, S. Krompiec, P. Lodowskie, A. Chrobok, Dalton Trans. 45 (2016) 1746;
(b) A.J. Amoroso, A. Banu, M.P. Coogan, P.G. Edwards, G. Hossain, K.M. Abdul Malik, Dalton Trans. 39 (2010) 6993;
(c) T. Auvray, B. Del Secco, A. Dubreuil, N. Zaccheroni, G.S. Hanan, Inorg. Chem. 60 (2021) 70.

[30] F.L. Thorp-Greenwood, M.P. Coogan, A.J. Hallett, R.H. Laye, S.J.A. Pope, J. Organometal. Chem. 694 (2009) 1400.

[31] (a) L. Wallace, D.P. Rillema, Inorg. Chem. 2 (1993) 3836;
(b) A. Juris, S. Campagna, L. Bidd, J.M. Lehn, R. Zeissel, Inorg. Chem. 27 (1988) 4007;
(c) L. Sacksteder, A.P. Zipp, E.A. Brown, J. Streich, J.N. Demas, B.A. DeGraff, Inorg. Chem. 29 (1990) 4335;
(d) M.S. Wrighton, D.L. Morse, J. Am. Chem. Soc. 96 (1974) 998.

[32] (a) E.M. Kober, T.J. Meyer, Inorg. Chem. 21 (1982) 3967;
(b) T.M. Stonelake, K.A. Phillips, H.Y. Otaif, Z.C. Edwardson, P.N. Horton, S. J. Coles, J.M. Beames, S.J.A. Pope, Inorg. Chem. 59 (2020) 2266;
(c) S.A. Fitzgerald, H.Y. Otaif, C.E. Elgar, N. Sawicka, P.N. Horton, S.J. Coles, J. M. Beames, S.J.A. Pope, Inorg. Chem. 60 (2021) 15467.

[33] (a) For example: V. Fernandez-Moreira, M.L. Ortego, C.F. Williams, M.P. Coogan, M.D. Villacampa, M.C. Gimeno Organometallics 31 (2012) 5950;
(b) L.C.-C. Lee, K.-K. Leung, K.K.-W. Lo, Dalton Trans. 46 (2017) 16357;
(c) R.G. Balasingham, F.L. Thorp-Greenwood, C.F. Williams, M.P. Coogan, S.J. A. Pope, Inorg. Chem. 51 (2012) 1419;
(d) A.J. Amoroso, M.P. Coogan, J.E. Dunne, V. Fernández-Moreira, J.B. Hess, A. J. Hayes, D. Lloyd, C. Millet, S.J.A. Pope, C. Williams, Chem. Commun. (2007) 3066;
(e) A.J. Amoroso, R.J. Arthur, M.P. Coogan, J.B. Court, V. Fernández-Moreira, A. J. Hayes, D. Lloyd, C. Millet, S.J.A. Pope, New J. Chem. 32 (2008) 1097;
(f) K.K.-W. Lo, M.-W. Louie, K.-S. Sze, J.S.-Y. Lau, Inorg. Chem. 47 (2008) 602.

[34] S.P. Schmidt, W.C. Trocler, F. Basolo, Inorg. Synth. 28 (1990) 160.

[35] (a) E.A. Stack, A.R. Day, J. Am. Chem. Soc. 65 (1943) 452;
(b) N.M. Shavaleev, H. Adams, J.A. Weinstein, Inorg. Chim. Acta 360 (2007) 700.

[36] J.S. Zakhari, I. Kinoyama, M.S. Dixon, A. Di Mola, D. Globisch, K.M. Janda, Bioorg. Med. Chem. 19 (2011) 6203.

[37] P. Laine, F. Bedioui, P. Ochsenbein, V. Marvaud, M. Bonin, E. Amouyal, J. Am. Chem. Soc. 124 (2002) 1364.

[38] S.J. Coles, P.A. Gale, Chem. Sci. 3 (2012) 683.

[39] (a) Rigaku, CrystalClear-SM Expert 3.1 b27, 2012; (b) Rigaku Oxford Diffraction, CrysAlisPro, v1.171.42.58a, 2022.

[40] G.M. Sheldrick, Acta Cryst. A64 (2008) (2008) 112.

[41] G.M. Sheldrick, Acta Crystallogr. Sect. C Struct. Chem. 71 (2015) 3.

[42] O.V. Dolomanov, L.J. Bourhis, R.J. Gildea, J.A.K. Howard, H. Puschmann, J. Appl. Cryst. 42 (2009) 339.